HUMAN GENE THERAPY 22:1575–1586 (December 2011)

DOI: 10.1089/hum.2011.070

Treatment of Advanced Leukemia in Mice with mRNA Engineered T Cells

David M. Barrett,[1,*] Yangbing Zhao,[2,*] Xiaojun Liu,[2] Shuguang Jiang,[2] Carmine Carpenito,[2] Michael Kalos,[2] Richard G. Carroll,[2] Carl H. June,[2,*] and Stephan A. Grupp[1,3,*]

Abstract

Cytotoxic T lymphocytes (CTLs) modified with chimeric antigen receptors (CARs) for adoptive immunotherapy of hematologic malignancies are effective in preclinical models and are being tested in several clinical trials. Although CTLs bearing stably expressed CARs generated by integrating viral vectors are efficacious and have potential long-term persistence, this mechanism of CAR expression can potentially result in significant toxicity. T cells were electroporated with an optimized *in vitro* transcribed RNA encoding a CAR against CD19. These RNA CAR CTLs were then tested *in vitro* and *in vivo* for efficacy. We found that T cells expressing an anti-CD19 CAR introduced by electroporation with optimized mRNA were potent and specific killers of CD19 target cells. CD19 RNA CAR T cells given to immunodeficient mice bearing xenografted leukemia rapidly migrated to sites of disease and retained significant target-specific lytic activity. Unexpectedly, a single injection of CD19 RNA CAR T cells reduced disease burden within 1 day after administration, resulting in a significant prolongation of survival in an aggressive leukemia xenograft model. The surface expression of the RNA CARs may be titrated, giving T cells with potentially tunable levels of effector functions such as cytokine release and cytotoxicity. RNA CARs are a genetic engineering approach that should not be subject to genotoxicity, and they provide a platform for rapidly optimizing CAR design before proceeding to more costly and laborious stable expression systems.

Introduction

Although a graft-versus-leukemia effect has been established in patients who undergo hematopoietic stem-cell transplant, suggesting acute lymphoblastic leukemia (ALL) may be controlled by cellular immune-mediated pathways, the relative lack of efficacy of donor lymphocyte infusion for ALL suggests that leukemic cells are poorly immunogenic. New methods that can overcome poor tumor immunogenicity and have the potential to be efficacious in ALL with less toxicity than standard approaches used in high-risk and relapsed disease, including stem-cell transplant, need to be pursued (Horowitz *et al*., 1990; Mehta 1993).

Chimeric antigen receptors (CARs) are molecules combining antibody-based specificity for tumor-associated surface antigens with T-cell receptor-activating intracellular domains with specific antitumor cellular immune activity (Eshhar *et al*., 1993; Eshhar, 1997; Brocker and Karjalainen, 1998). These CARs allow a T cell to achieve major histocompatibility complex–independent primary activation through single-chain variable fragment (scFv) antigen-specific extracellular regions fused to intracellular domains that provide T-cell activation and costimulatory signals. Second- and third-generation CARs also provide appropriate costimulatory signals via CD28 and/or CD137 (4-1BB) intracellular activation motifs, which augment cytokine secretion and antitumor activity in a variety of solid-tumor and leukemia models (Pinthus *et al*., 2004; Milone *et al*., 2009; Sadelain *et al*., 2009).

Most investigators have obtained efficient CAR gene transfer into human T cells via retrovirus or HIV-derived lentivirus for human tumor and HIV antigens, with some of these cell-therapy products advancing in phase I/II trials (Deeks *et al*., 2002; Kershaw *et al*., 2006; Pule *et al*., 2008; Till *et al*., 2008). Recently, our group has reported on the use of CD19-targeted CAR^+ T cells in three patients with chronic lymphoblastic leukemia (Kalos *et al*., 2011; Porter *et al*., 2011). Two of these patients with refractory disease and very large

[1]Division of Oncology, Children's Hospital of Philadelphia, Philadelphia, PA 19104.
[2]Abramson Family Cancer Research Institute, University of Pennsylvania Cancer Center, Philadelphia, PA 19104.
[3]Department of Pathology, Children's Hospital of Philadelphia, Philadelphia, PA 19104.
*D.M.B, Y.Z., C.H.J., and S.A.G. contributed equally to this work.

disease burdens entered a complete remission after 4 weeks. These responses have been sustained and the CAR^+ T cells persistent for >6 months, suggesting the efficacy of this approach. Approaches using integrating viral vectors have clear advantages, including long-term expression of the CAR on infused cells across multiple cell divisions. However, iterative clinical trials that rapidly incorporate CAR design innovations are difficult to implement using viral vectors, because of the complexity of release testing and the high expense of vector production. In addition, there is the regulatory concern that use of integrating viral vectors might result in insertional mutagenesis. This has clearly been seen in the case of a retroviral vector used in gene modification of hematopoietic stem cells in the treatment of X-linked severe combined immunodeficiency (Hacein-Bey-Abina *et al*., 2008). In the case of lentiviral vectors, or in the setting of gene modification of mature lymphocytes, this is a theoretical concern, but it is an issue for regulators of gene- and cell-therapy approaches.

Electroporation-mediated mRNA transfection is a potentially complementary approach for gene expression that does not result in permanent genetic modification of cells. The use of mRNA for gene-therapy applications was first described by Malone and co-workers in the context of liposome-mediated transfection (Malone *et al*., 1989). Successful electroporation of mRNA into primary T lymphocytes has now been developed and used for efficient T-cell receptor (TCR) gene transfer (Y. Zhao *et al*., 2005, 2006). More recently, CARs against the Her2/neu antigen were introduced into T cells by mRNA electroporation and were found to be more effective than Her2/neu antibodies in a breast cancer xenograft model (Yoon *et al*., 2009). Other human target antigens of CARs introduced into T cells by mRNA electroporation include carcinoembryonic antigen and ErbB2 (Birkholz *et al*., 2009). Although a number of studies have demonstrated efficacy using this approach in solid tumors after intratumoral injection or in local injection intraperitoneal models, no group has demonstrated similar success in disseminated leukemia preclinical models, possibly due to the difficulty in generating efficacy in a disseminated model with a transient expression system (Rabinovich *et al*., 2009). In comparison with long-term (integrating) expression systems, mRNA transfection would allow more rapid iterative changes in CAR design to move into a GMP-compliant system. Manufacturing costs are far less. Release testing is less complex. In settings where long-term expression is required for clinical efficacy and repeated cell infusion not possible, the mRNA approach would not be suitable. However, for initial testing of antigens where "on-target, off-tissue" toxicity (Morgan *et al*., 2010) might be a risk, transient expression could potentially allow for greater safety in initial CAR testing.

CD19 is a surface antigen restricted to B cells and is expressed on early pre-B cells and a majority of B-cell leukemias and lymphomas (Nadler *et al*., 1983). This makes CD19 an attractive antigen for targeted therapy, as it is expressed on the malignant cell lineage and a specific subset of early and mature B lymphocytes, but not hematopoietic stem cells. It has been postulated that CD19 depletion allows for eventual restoration of a normal B-cell pool from the CD19-negative precursor population (Cheadle *et al*., 2010). Experience with rituximab, the anti-CD20 monoclonal antibody used for treatment of B-cell malignancies and autoimmune disorders, has shown that therapy-induced B-cell deficiency is well tolerated (Plosker and Figgitt, 2003; van Vollenhoven *et al*., 2010). We hypothesized that transient anti-CD19 CAR expression via mRNA transfection would provide effective adoptive T-cell therapy for leukemia without risk of permanent genetic modification of the effector cell, and tested this novel approach by using a robust mouse xenograft model of disseminated leukemia as a therapeutic intervention.

Materials and Methods

Construction of in vitro *transcription (IVT) vectors and RNA electroporation*

CD19 and mesothelin (meso)-targeted CARs with 4-1BB and CD3ζ signaling domains (19-BBz and ss1-BBz, respectively) have been described previously (Carpenito *et al*., 2009; Milone *et al*., 2009). The PCR products were subcloned into pGEM.64A-based vector by replacing green fluorescent protein (GFP) from pGEM-GFP.64A (Y. Zhao *et al*., 2006) with restriction enzyme-digested PCR products with *Hin*dIII and *Not*I to produce pGEM-ss1.bbz.64A and pGEM-CD19bbz.64A. Similarly, third-generation versions of the CARs were constructed by using the CD28-signaling domain. The replaced CAR cDNAs were confirmed by direct sequencing and linearized by *Spe*I digestion prior to RNA IVT. mScript RNA System (Epicentre, Madison, WI) was used to generate capped IVT RNA. The IVT RNA was purified using an RNeasy Mini Kit (Qiagen, Inc., Valencia, CA), and purified RNA was eluted in RNase-free water at 1–2 mg/ml. Human T cells were stimulated by CD3/CD28 beads as described (Carpenito *et al*., 2009). The stimulated T cells were washed three times with Opti-MEM and resuspended in Opti-MEM at the final concentration of $1–3\times10^8$/ml prior to electroporation. Subsequently, the stimulated T cells were mixed with 10 μg/0.1 ml T cells of IVT RNA (as indicated) and electroporated in a 2-mm cuvette (Harvard Apparatus BTX, Holliston, MA) using an ECM830 Electro Square Wave Porator (Harvard Apparatus BTX). Viability post transfection ranged from 50% to 80%, and in all cases viable T cells for injection had >99% CAR expression at the time of use. For the trafficking experiments, T cells were stably transduced with a firefly luciferase lentiviral construct prior to mRNA transfection.

Construction of lentiviral vectors with different CARs. Lentiviral vectors that encode the various CARs under the transcriptional control of the EF-1α promoter were generated as previously described (Imai *et al*., 2004; Milone *et al*., 2009). CAR-expressing lentiviral vectors in which the CAR sequences were preceded in frame by either an eGFP sequence or firefly luciferase followed by the 2A ribosomal skipping sequence from foot-and-mouth disease virus were also generated. These vectors permit dual expression of GFP or firefly luciferase and the CARs from a single RNA transcript. All constructs were verified by sequencing.

CAR detection on electroporated T cells

Cells were washed and suspended in FACS buffer (PBS with 0.1% sodium azide and 0.4% bovine serum albumin). Cells were incubated at 4°C for 25 min with biotin-labeled

polyclonal goat anti-mouse F(ab)2 antibodies (anti-Fab; Jackson Immunoresearch, West Grove, PA) and then washed twice with FACS buffer. Cells were then stained with phycoerythrin (PE)-labeled streptavidin (BD Pharmingen, San Diego, CA). Flow-cytometry acquisition was performed with a BD FACSCalibur (BD Biosciences), and analysis was performed with FlowJo (Treestar Inc., Ashland, OR).

ELISA and Luminex assays

Target cells were washed and suspended at 10^6 cells/ml in C10 (RPMI 1640 supplemented with 10% fetal calf serum; Invitrogen). Target cells (10^5) of each type were added to each of two wells of a 96-well round-bottom plate (Corning). Effector T-cell cultures were washed and suspended at 10^6 cells/ml in C10. Effector T cells (10^5) were combined with target cells in the indicated wells of the 96-well plate. In addition, wells containing T cells alone were prepared. The plates were incubated at 37°C for 18–20 hr. After the incubation, an ELISA assay was performed on the supernatant using the manufacturer's instructions (Pierce, Rockford, IL). Fifty microliters of culture supernatant were tested in duplicate, and the results reported in picograms per milliliter.

CD107a staining

Cells were plated at an effector:target ratio (E:T) of 1:1 (10^5 effectors:10^5 targets) in 160 μl of C10 medium in a flat-bottom 96-well plate. Controls included wells without target cells to assess background levels of CD107a. Twenty microliters of PE-labeled anti-CD107a Ab (BD Pharmingen) was added; the plate was gently agitated and incubated at 37°C for 1 hr. GolgiStop solution was added and plates incubated for another 2.5 hr. Cells were then stained with 10 μl of fluorescein isothiocyanate–anti-CD8 and allophycocyanin–anti-CD3 (BD Pharmingen) and washed. Flow-cytometry acquisition was performed with a BD FACSCalibur (BD Biosciences), and analysis was performed with FlowJo (Treestar Inc.).

Flow-cytometric cytotoxic T-lymphocyte assay

A slightly modified version of a flow-cytometric cytotoxicity assay was used (Hermans *et al.*, 2004). In this assay, the cytotoxicity of target cells is measured by comparing survival of target cells relative to the survival of negative control cells within the same tube as the effector cells. In our experiments, the target cells were K562 cells expressing human CD19 (K562-CD19), and the negative control cells were K562 cells expressing mesothelin (K562-meso). K562-meso were labeled with the fluorescent dye 5-(and-6)-(((4-chloromethyl) benzoyl)amino)tetramethylrhodamine (CMTMR; Invitrogen). K562-CD19 cells were labeled with carboxyfluorescein diacetate succinimidyl ester (CFSE) (Invitrogen). Cultures were set up in 96-well culture plate in duplicate at the following T cell:target cell ratios: 10:1, 3:1, and 1:1, using 10^4 $CD19^+$ target cells and 10^4 $meso^+$ control cells. For some experiments in which both K562-CD19 and K562-meso were used as target cells and were labeled with CFSE, a myeloma cell line NSO that is negative for CD19 was labeled with CMRA as a negative control. The cultures were incubated for 4 hr at 37°C. Immediately after the incubation, 7-aminoactinomycin D (7-AAD) (BD Pharmingen) was added as recommended by the manufacturer. Analysis was gated on 7-AAD-negative (live) cells, and the percentages of live K562-CD19 and live K562-meso cells were determined for each T cell + target cell culture. For each culture, the percent survival of K562-CD19 was determined by dividing the percent live K562-CD19 cells by the percent live K562-meso control cells. The corrected percent survival of K562-CD19 was calculated by dividing the percent survival of K562-CD19 cells in each T cell + target cell culture by the ratio of the percent K562-CD19 target cells:percent K562-meso negative control cells in tubes containing only K562-CD19 target cells and K562-meso negative control cells without any effector T cells. This correction was necessary to account for variation in the starting cell numbers and for spontaneous target cell death. Cytotoxicity was calculated as 100% (corrected percent survival of K562-CD19). For all E:T ratios, the cytotoxicity was determined in duplicate and the results were averaged.

Mouse xenograft studies

Studies were performed as previously described with certain modifications (Teachey *et al.*, 2006, 2008). In brief, 6–10-week- old NOD-SCID-$\gamma c^{-/-}$ (NSG) mice were obtained from the Jackson Laboratory (Bar Harbor, ME) or bred in house under an approved institutional animal care and use committee protocol and maintained under pathogen-free conditions. The $CD19^+$ human ALL line Nalm-6 was obtained from American Type Culture Collection (ATCC; Manassas, VA). Animals were injected via the tail vein with 10^6 viable Nalm-6 cells in 0.2 ml of sterile PBS. T cells were injected via the tail vein at 5×10^6, 1×10^7, or 2.5×10^7 cells in a volume of 0.2 ml of sterile PBS 7 days after injection of Nalm-6. Nalm-6 at this dose reliably produces fatal leukemia in the NSG mouse in 22–25 days if left untreated. Previous experiments demonstrated that the earliest reliable detection of disease ($>0.1\%$) in femoral bone marrow was 7 days after injection, and thus this time point is chosen for therapeutic intervention and correlated with bioluminescent disease. Animals were closely monitored for signs of graft-versus-host disease and other toxicity as evidenced by $>10\%$ weight loss, loss of fur, diarrhea, or conjunctivitis, as well as for leukemia-related hind-limb paralysis. Peripheral blood was obtained by retro-orbital bleeding, and the presence of ALL and T-cell engraftment was determined by flow cytometry using BD TruCOUNT (BD Biosciences) tubes as described in the manufacturer's instructions. CD19, CD20, CD4, CD3, CD10, and/or CD8 expression (as required) was detected by staining with fluorescently-conjugated monoclonal antibodies (BD Biosciences). Expression of the CD19 or SS1 scFv CARs was detected using the biotinylated F(ab')2 fragment from goat anti-mouse IgG sera (specific for scFvs of murine origin) (Jackson ImmunoResearch), followed by staining with streptavidin-PE (BD Biosciences/Pharmingen).

Bioluminescent imaging

Anesthetized mice were imaged using a Xenogen Spectrum system and Living Image v4.0 software. Mice were given an intraperitoneal injection of 150 mg/kg D-luciferin (Caliper Life Sciences, Hopkinton, MA). Previous titration of both Nalm-6 and human T cells transduced with the firefly luciferase vector indicated time to peak of photon emission to be 5 min, with peak emission lasting for 6–10 min. Each animal was imaged alone (for photon quantitation) or in

groups of up to five mice (for display purposes) in the anterior–posterior prone position at the same relative time point after luciferin injection (6 min). Data were collected until the mid range of the linear scale was reached (600–60,000 counts) or maximal exposure settings reached (f stop 1, large binning, and 120 sec), and then converted to photons/second/cm^2/steradian to normalize each image for exposure time, f stop, binning, and animal size. For anatomic localization, a pseudocolor map representing light intensity was superimposed over the grayscale body-surface reference image. For data display purposes, mice without luciferase-containing cells were imaged at maximal settings, and a mean value of 3.6×10^5 p/sec/cm^2/sr was obtained. Mice with luciferase-containing Nalm-6 typically became moribund with leukemia when photon flux approached 5×10^{11} p/sec/cm^2/sr, giving a detection range of 6 orders of magnitude. Similarly, luciferase-expressing versions of the various CARs were used to detect trafficking of the T cells to tumor sites and to assess expansion of the transferred T cells in the host mouse.

Cell-line identity testing

Nalm-6 and K562 parent cell lines were obtained from ATCC and genotyped by short tandem repeat analysis (Masters *et al*., 2001). Cell lines were verified every 6 months, or after any genetic modification such as CD19 or luciferase transduction, to insure identity.

Statistical considerations

Analysis was performed with STATA version 10 (Statacorp, College Station, TX) or Prism 4 (Graphpad Software, La Jolla, CA). *In vitro* data represent means of duplicates, and comparisons of means were made via the Mann-Whitney test. For comparison among multiple groups, Kruskal-Wallis analysis was performed with Dunn multiple comparison tests to compare individual groups. Survival curves were compared using the log-rank test with a Bonferroni correction for comparing multiple data sets.

Results

Generation of CAR-expressing T cells by mRNA transfection results in up to 10 days of surface expression with detectable lytic activity

We evaluated the persistence of expression and cytolytic activity of mRNA-transfected CAR^+ CTLs (RNA CARs) *in vitro*. High surface expression persisted for 6 days *in vitro* before drifting down toward baseline nonexpressing cells by 10 days (Fig. 1A and data not shown). This prolonged high transgene persistence was different from most reports of peak and duration of expression of a surface antigen after mRNA transfection (Birkholz *et al*., 2009; Rabinovich *et al*., 2009; Yoon *et al*., 2009; Li *et al*., 2010), possibly due to our optimized IVT vector and RNA production (data not shown). In parallel, we assessed the cytotoxic potential of CAR-expressing T cells *in vitro* with a flow cytometry–based killing assay. Specific lysis of >50% of target cells at an E:T ratio of 2:1 was noted from days 1 to 4. Although cytotoxic activity declined on days 5–6, even with a 2–3-log reduction in surface expression of the CAR, some lytic activity was observed and was well over that of background lysis of mock-transfected cells (Fig. 1B). Specific lytic activity declined in parallel with declining mean fluorescent intensity (MFI) of the expressed transgene, but significant lytic activity ($p<0.05$) over nonelectroporated controls at an E:T ratio of 20:1 was observed 6 days after electroporation.

To further assess the lytic activity of the RNA CAR^+ T cells, they were stimulated and electroporated as above, then cocultured with various target cells 4 hr after electroporation to examine cytolytic potential and target specificity. We used expression of CD107a as a marker of cytolytic cell degranulation (Betts and Koup, 2004). In addition to our target of interest (CD19), we used a CAR directed against the irrelevant antigen mesothelin (not expressed on lymphocytes) as a control. K562 cells express neither CD19 nor mesothelin, but are easily transduced to express a variety of genes, making them flexible target cells for *in vitro* cytotoxicity assessments (Suhoski *et al*., 2007). CD19-directed RNA CAR^+ T cells degranulate and express CD107a only in the presence of $CD19^+$ target, indicating antigen-specific recognition and lytic function (Fig. 1C). This included both the $CD19^+$ target leukemia cell line Nalm-6 and K562 cells transduced to express CD19. As a control, CAR recognizing mesothelin only specifically lyse $mesothelin^+$ K562 cells, as measured by the same CD107a assay. Mesothelin-directed CAR^+ T cells do not express CD107a in the presence of $mesothelin^-$ parent K562, the $CD19^+$/$mesothelin^-$ ALL line Nalm-6, or K562 transduced to express surface CD19, but not mesothelin. A coculture experiment using both an anti-meso CAR with 4-1BB and TCR ζ signaling domains (BBz) and an anti-CD19-BBz CAR also demonstrated specific release of interleukin-2 (IL-2) in the presence of appropriate target as measured by ELISA of the supernatant, suggesting antigen-specific T-cell activation (Fig. 1D).

Relationship of CAR expression level to input RNA dose

Recent reports of serious adverse events after administration of CAR T cells engineered by retroviral gene transfer (Brentjens *et al*., 2010; Morgan *et al*., 2010) suggest that a platform for expressing CARs with predetermined levels of surface expression or which ensures self-limited expression (such as RNA) might be desirable. By titrating the mRNA dose, an approximately 100-fold variation of RNA CAR surface expression by MFI is observed (Fig. 2A). Despite the variation in surface MFI, the rate of decline of expression (expressed as percentage) is similar (Fig. 2B). RNA CAR^+ T cells exhibit similar lytic activity on day 1 post electroporation (Fig. 2C, left panel) and secretion of interferon-γ (IFN-γ) (Fig. 2D). Secretion of IL-2 was also tested (data not shown). This is consistent with a recent report using a different methodology (James *et al*., 2010). By day 3, however, a dose-dependent decline in lytic activity is observed where lower RNA doses are less effective compared with their effects on day 1, whereas higher doses (40 and 20 μg) have similar lytic profiles at each E:T ratio on day 3 as on day1. This suggests that the initial surface expression, which appears proportional to the input RNA, could dictate the time and degree of lytic activity. This may be useful in controlling the duration of effect and potentially the duration of cytokine release, although this remains to be studied.

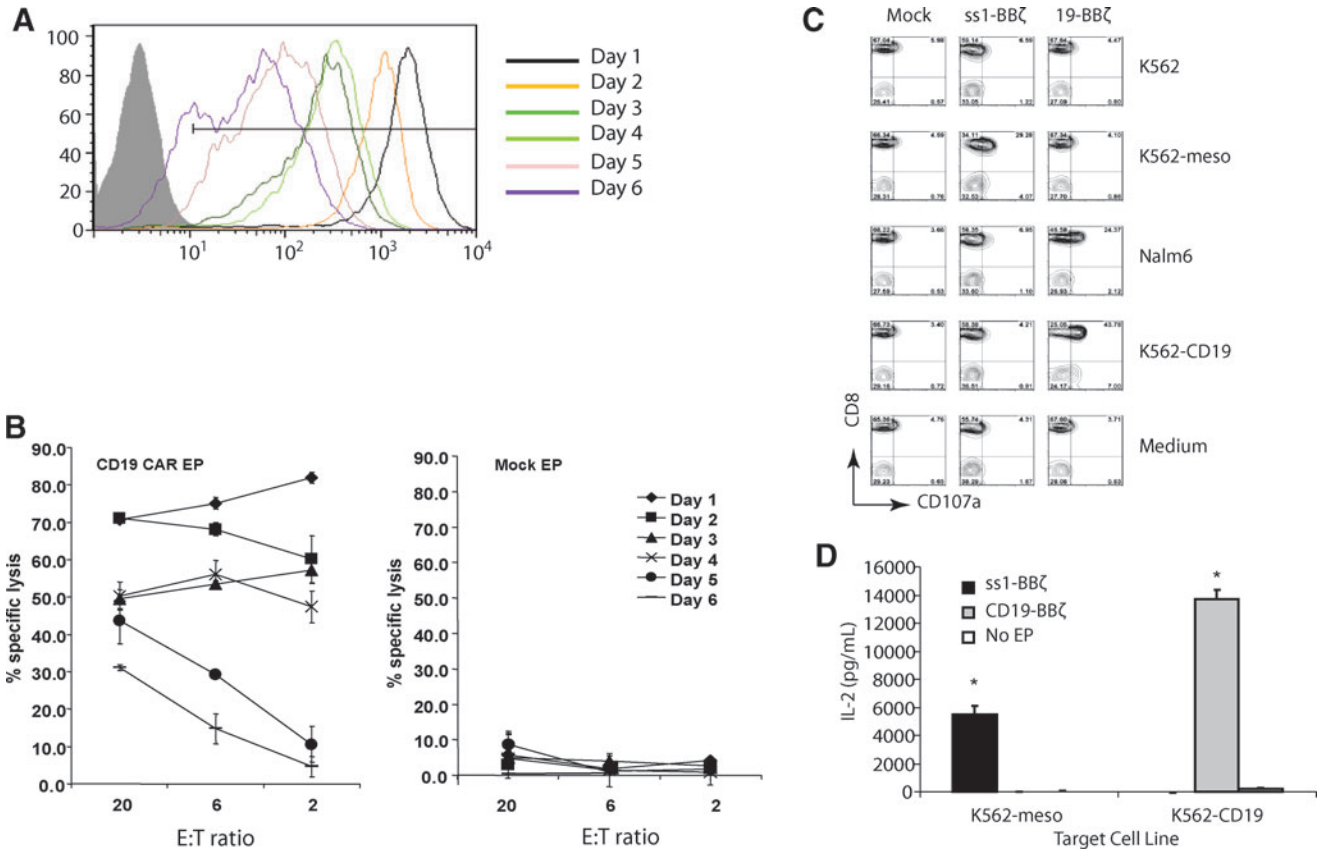

FIG. 1. Optimized mRNA electroporation procedure results in uniform high-level surface expression and specific function of CAR T cells *in vitro*. **(A)** CAR expression as measured by mean fluorescent intensity (MFI) at different time points after electroporation with CD19-BBz mRNA in anti-CD3 and CD28 stimulated peripheral blood T cells (open histograms). Nonelectroporated T cells were used as negative control (filled histogram). **(B)** RNA CAR$^+$ T cells specifically kill CD19 targets. A flow-based CTL assay was conducted on the indicated day post electroporation with K562-CD19 as target and K562-meso as control (data not shown). **(C)** Peripheral blood lymphocytes (PBLs) were electroporated with ss1-BBz, CD19-BBz, or no mRNA (Mock). Four hours post electroporation, the T cells were cocultured with K562, NALM-6, or K562 expressing either CD19 (K562-CD19) or mesothelin (K562-meso) and analyzed for CD107a staining. CD3$^+$ T cells were gated. Only antigen-specific CD107a expression is observed. **(D)** Four hours post electroporation, T cells electroporated with mRNA encoding for CD19-BBz or ss1-BBz were cocultured with K562-meso or K562-CD19 target cells for 16 hr. IL-2 production was measured in the supernatant by ELISA, with significant increases in IL-2 production in an antigen-specific manner ($^*p < 0.01$). Data are representative of at least two independent experiments.

In vivo *trafficking of CAR$^+$ CTLs*

Based on the above *in vitro* data demonstrating RNA CAR expression for up to a week, we assessed the cytolytic function of mRNA-transfected CAR$^+$ T cells after 48 hr in a xenograft mouse model. We were curious to see if the lack of any reported success with RNA CARs against disseminated CD19 was related to a loss of function after infusion, whether through poor trafficking to target sites or faster than expected loss of receptor expression. NSG mice were inoculated by tail vein with the CD19$^+$ ALL line Nalm-6 7 days prior to infusion of 10^7 19-BBz or anti-meso (SS1)-BBz RNA CAR$^+$ T cells (Fig. 3). Mice were sacrificed 48 hr after T-cell infusion, and T cells were recovered and enriched from peripheral blood, spleen, femoral bone marrow, and a peritoneal washing using a negative selection protocol. After 48 hr of *in vivo* proliferation and exposure to a CD19$^+$ Nalm-6 target, T cells expressing the CAR could still be detected in peripheral blood, spleen, and peritoneum. Surface anti-CD19 CAR expression is modestly lower than that of companion control cultured T cells *in vitro* (Fig. 3A). Meso-BBz CAR T cells that had not been exposed to targets expressing the cognate mesothelin surrogate antigen were also recovered from these compartments. The overall CAR$^+$ populations from the spleen were 75% (as a percentage of total human CD3$^+$ cells recovered) for CD19 and 68% for mesothelin at this time point. So although the CD19 CAR CTLs were expanding based on bioluminescence (Fig. 4) and the mesothelin CAR CTLs were not, the proliferating CD19 CAR CTLs appear to be producing CAR$^+$ progeny. If CAR-mediated proliferation were resulting in CAR$^-$ progeny, the percentage of CD19 CAR$^+$ cells should be lower than that for the nonproliferating mesothelin CAR CTLs. Few human CD3$^+$ cells for either construct were recovered from femoral bone marrow at this time point, likely due in part to the diluted distribution of T cells throughout unaccessible regions of marrow (vertebral bodies, calvarium). The goat anti-mouse IgG serum used to stain for the CAR also cross-reacts with many bone marrow precursor cells, giving a high background in the evaluation of this compartment.

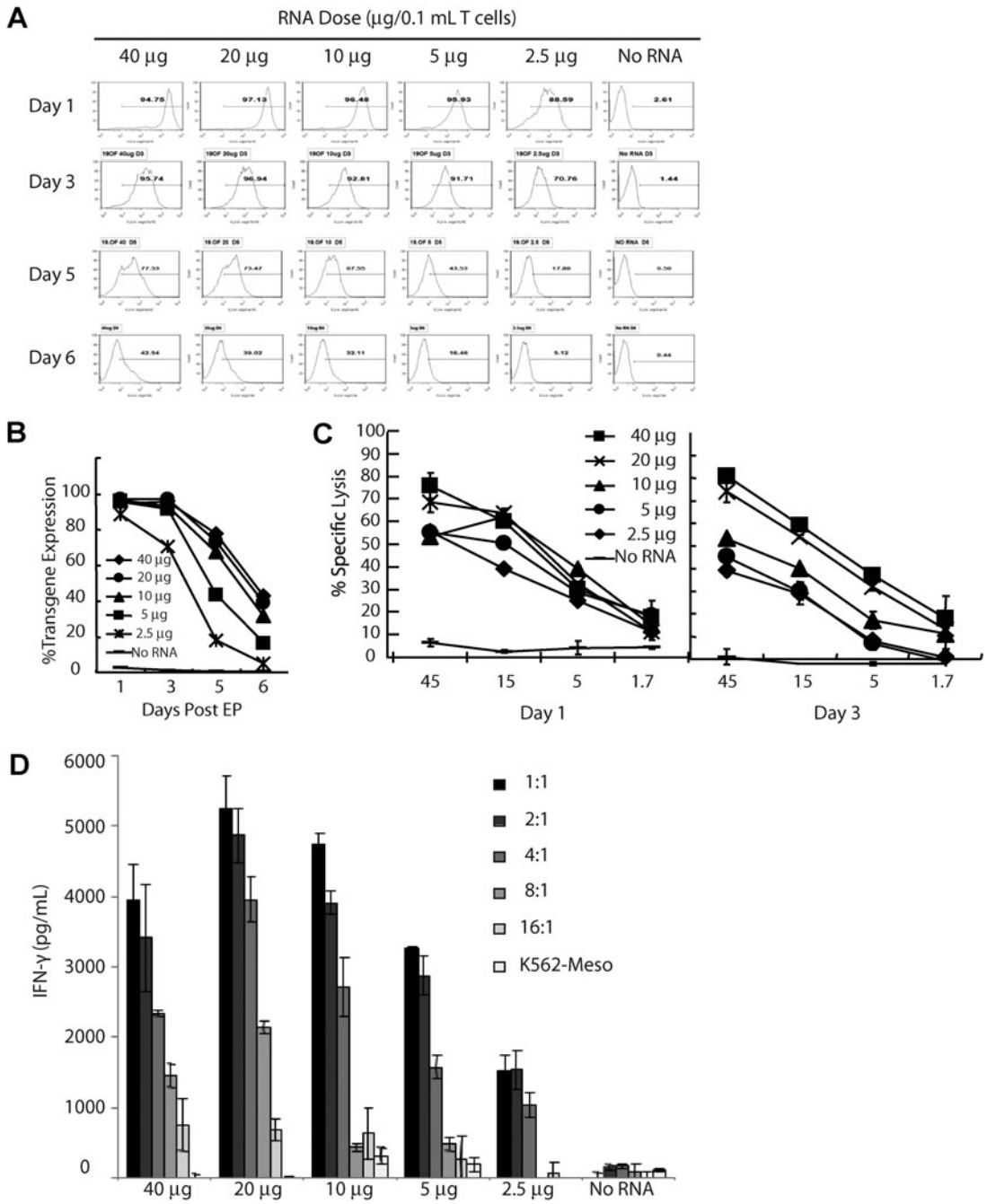

FIG. 2. Potentially tunable transgene expression and effector functions of RNA CAR$^+$ T cells. **(A)** Transgene expression of RNA CAR$^+$ T cells electroporated with the indicated amounts of CD19-BBz RNA plotted as a function of time. Histograms of transgene expression of electroporated 19-BBz CAR mRNA are shown. **(B)** Transgene expression data from (A) plotted as a line graph. Rate of decline is similar despite different MFI seen in (A). **(C)** Specific lysis of CD19$^+$ tumor cells with CAR T cells electroporated with the indicated amounts of RNA. Lysis was measured by a flow-cytometric CTL assay using K562-CD19 as targets on day 1 (*left panel*) and day 3 (*right panel*) after electroporation. Although little difference exists on day 1, by day 3 a dose-dependent decrease in specific lysis relative to RNA dose is observed. **(D)** IFN-γ secretion by CAR T cells (4 hr after electroporation) with the indicated amounts of RNA cocultured overnight with serially diluted target cells (K562-CD19) or control targets (K562-meso at 1:1) assayed by ELISA. IFN-γ secretion titrates with the amount of target, and is not statistically significantly different among CD19 CAR$^+$ groups, although a trend toward lower cytokine secretion with lower RNA doses is suggested.

We used cells recovered from the 48-hr peritoneal washings, which had the most human CD3$^+$ and CAR$^+$ enriched population regardless of whether the T cells were administered intraperitoneally (IP) or intravenously (IV), for further *in vitro* characterization. T cells recovered from the peritoneum of mice 48 hr after injection of 10^7 CAR$^+$ T cells were tested for antigen-specific cytotoxicity in a flow cytometry–based CTL assay (Fig. 3B). Significant antigen-specific target lysis was obtained with RNA CAR$^+$ T cells recovered from mice after 48 hr, comparable to those that were cultured *in vitro* for 48 hrs.

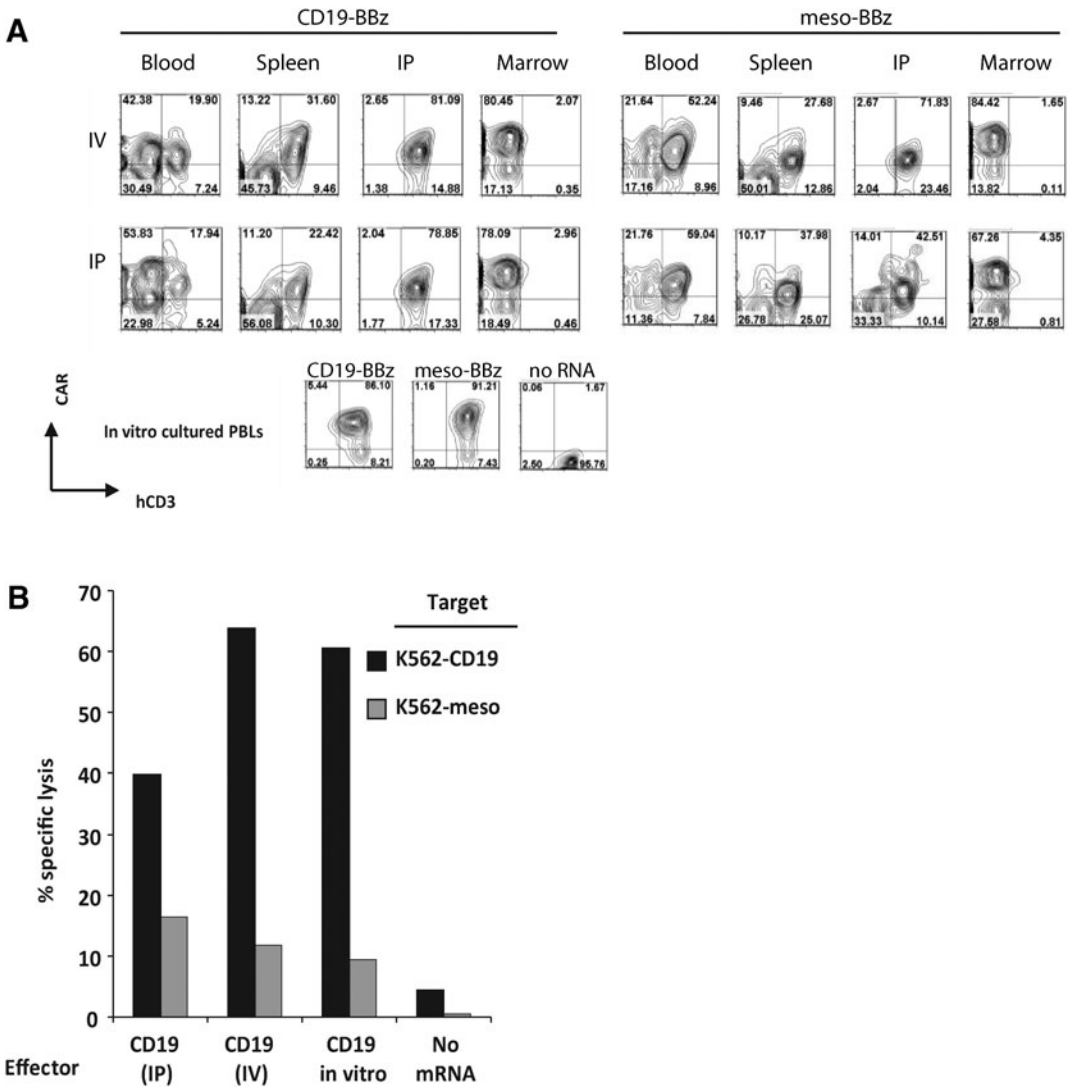

FIG. 3. Expression and function of RNA CARs *in vivo*. **(A)** NOD/SCID/$\gamma c^{-/-}$ null (NSG) mice were injected with 10^7 PBLs either intravenously (IV) or intraperitoneally (IP) 4 hr after electroporation with ss1-BBz or CD19-BBz. Mice were sacrificed after 48 hr, and human PBLs were isolated from peripheral blood, spleen, bone marrow, and intraperitoneal washing (IP) by using a T cell negative selection kit (Dynal Magnetic Beads). The purified cells were stained for human CD3 and CAR expression (via a panspecific goat anti-mouse IgG) and analyzed by flow cytometry. Significant background staining of mouse marrow precursor cells is observed in the bone-marrow compartment despite negative selection. $CD3^+CAR^+$ cells are recovered from blood, spleen, and a peritoneal washing, but rarely from the femoral bone marrow at this time point. **(B)** Purified T cells recovered from intraperitoneal washings 2 days after injection of mice by the IV or IP route with CD19-BBz were used in a flow-based CTL assay. CD19-BBz RNA electroporated T cells that had been cultured *in vitro* for 2 days (CD19 in vitro) and mock electroporated T cells (No mRNA) were used as controls. The graph shows percent lysis of the purified PBLs against K562-CD19 or K562-meso targets. Target-specific lysis observed in recovered CAR CTLs is comparable to that of *in vitro* cultured CAR^+ PBLs and is significantly higher than no mRNA controls ($p < 0.01$).

Next, we evaluated the anatomic distribution of RNA CAR CTLs for 3 days using *in vivo* bioluminescence. Mice were infused with Nalm-6 and, on day 7, with 5×10^6 RNA CAR^+ T cells (50% $CD4^+$ and 50% $CD8^+$, both IV). To evaluate the effects of antigen recognition and CAR signaling on biodistribution, we compared RNA CAR^+ T cells expressing 19-BBz and ss1-BBz, as well as mock-transfected T cells. We used T cells that were stably transduced with a firefly luciferase lentiviral construct prior to mRNA transfection to allow for *in vivo* bioluminescent tracking and relative quantitation. Retention at sites of disease and subsequent proliferation as indicated by increasing total bioluminescent signal, as well as heat maps over known disease sites, required recognition of a target antigen (Fig. 4). T cells with CARs against antigens not present in the model (mesothelin) or mock-transfected cells concentrated in the spleen and showed no increase in bioluminescence over time from injection. The lack of increase of bioluminescence activity suggests a lack of T-cell expansion *in vivo* as luminescent signal is directly proportional to cell number (H. Zhao *et al.*, 2005; Dobrenkov *et al.*, 2008). T cells with 19-BBz migrated to, were retained, and proliferated at sites of disease (axial skeleton, femoral bone marrow, spleen, and likely the liver in the right flank) (Fig. 4B). In addition, the total bioluminescent

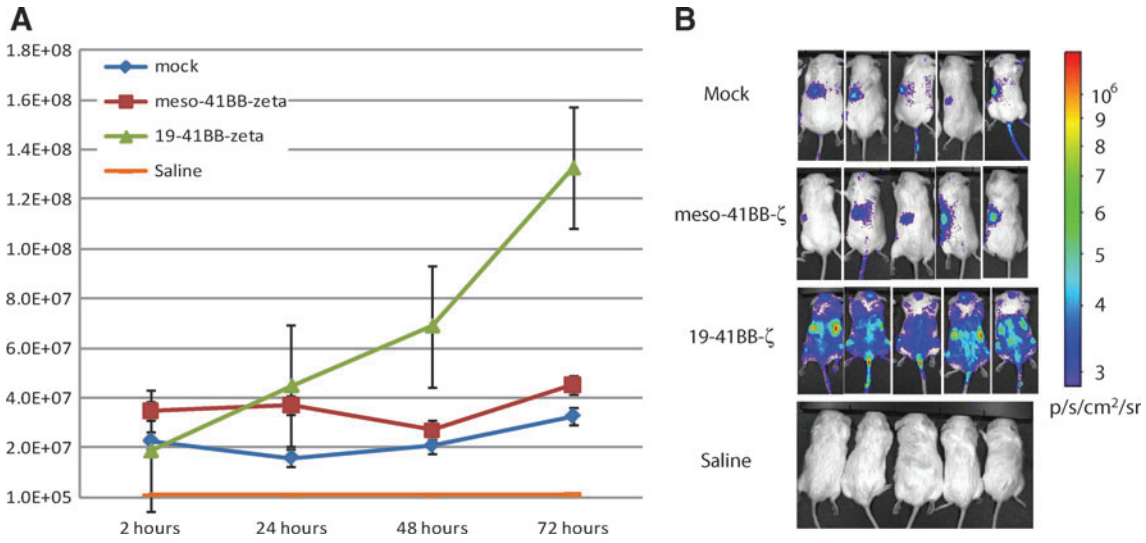

FIG. 4. Specific trafficking and proliferation of RNA CARs in tumor-bearing mice. **(A)** NOD/SCID/$\gamma c^{-/-}$ (NSG) mice were injected IV with 10^6 Nalm-6 cells followed 7 days later with 5×10^6 T cells 4 hr after electroporation with the indicated mRNA constructs. The T cells had been stably transfected with a lentiviral construct to express firefly luciferase, and mice were imaged for bioluminescence. The graph indicates average of individual total photon flux ± the standard error for each of the indicated groups ($n=8$). **(B)** CD19 RNA CARs exhibit increasing bioluminescence signal and anatomic distribution consistent with migration to sites of disease and CAR T-cell proliferation. Photon density heat maps on day 3 post injection suggest that mock T cells or T cells expressing RNA CARs with irrelevant specificity against mesothelin pool passively in the spleen (left flank on heat map) and do not increase in photon density, indicating a lack of proliferation. Note that the 5×10^6 cells produce a p/sec/cm^2 flux of $\sim2\times10^7$, equivalent among all groups immediately after injection. Saline-treated mice represent the background autoluminescence of 5×10^5 p/sec/cm^2.

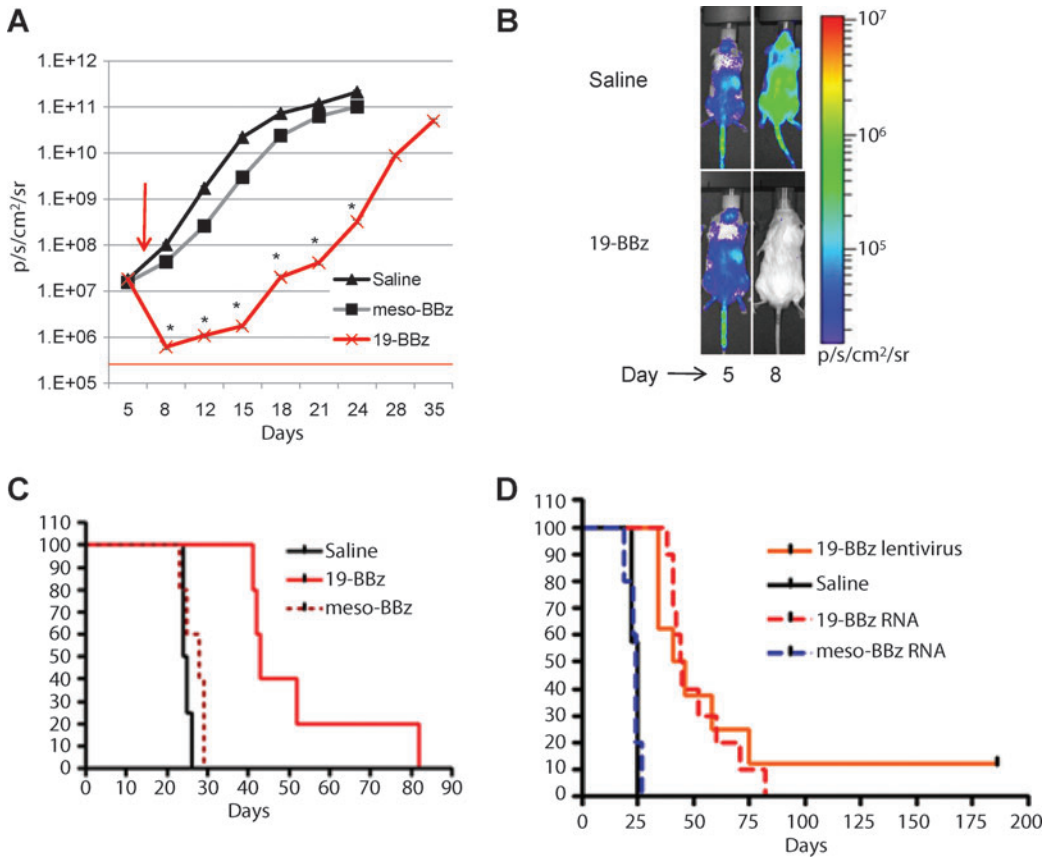

signal increased over the whole mouse, as well as sites of known involvement by Nalm-6, consistent with proliferative expansion of the T-cell number (Fig. 4A). A time-course experiment with Nalm-6 stably transduced with firefly luciferase revealed that disease is present in the same locations (axial skeleton, femoral bone marrow, spleen, and liver), and that a 4-log increase in bioluminescent signal corresponded to an increasing disease burden (Supplementary Fig. S1; Supplementary Data are available online at www.liebertonline.com/hum). Consistent with previous experiments, there were few, if any, CTLs present in the peripheral blood compartment during the initial 3 days after T-cell injection, with <10 human T cells/μl detected by TruCOUNT quantitation, whereas large numbers of human T cells are detected in the peripheral blood at later time points (data not shown). Similarly, the appearance of Nalm-6 in the peripheral blood is a late event in this model, with mice showing <10 human ALL cells/μl of peripheral blood until shortly before the animals become moribund, typically by day 21 (data not shown). Over multiple repeats of this experimental model, this remains the consistent finding, highlighting the sensitivity of bioluminescence over traditional evaluation using flow cytometry to quantify CTLs or blasts in the peripheral blood.

In vivo *efficacy of CAR$^+$ CTLs against CD19$^+$ ALL in a xenograft model*

In order to assess potential *in vivo* efficacy of RNA CAR CTLs, animals were treated as before, but given a single higher dose of T cells (2.5×10^7) on day 7 post tumor inoculation. We chose a dose of 2.5×10^7 instead of 10^7 cells by hypothesizing that, as the receptor expression was self-limited to a few days, the CAR-driven expansion of cells would similarly be limited and a higher starting cell dose might be required to demonstrate efficacy in a high tumor burden. Preclinical models using stably transduced CD19 CAR$^+$ T cells with retroviruses have used a schedule of three or four separate injections with $3–4\times10^7$ total T cells in similar models (Brentjens *et al.*, 2007; Shaffer *et al.*, 2011). We were surprised to observe a 2-log reduction of bioluminescent signal as early as 24 hr after injection, a reduction that was sustained over time ($p<0.01$; Fig. 5A). The bioluminescence signal was globally reduced, without evidence of a reservoir that the CTLs fail to penetrate (Fig. 5B), although signal never reached undetectable levels, indicating it was not cleared entirely. Of note, two-dimensional heat maps are not capable of separating CNS disease from other sites, so we undertook *ex vivo* imaging of the brain, skull, spine, and vertebrae, which revealed that the CNS appears not significantly involved at this time point (day 5). Rather, the calvarium/skull base and vertebral bodies are involved with leukemia, giving rise to the heat maps over the head and back of the mouse (data not shown). This is consistent with other reports of the early migration of human hematopoietic cells in immunodeficient mice evaluated by optical imaging (Kalchenko *et al.*, 2006). Mesothelin-directed CAR CTLs had no significant effect on bioluminescent disease burden, indicating little nonspecific allogeneic or xenogeneic effect. The initial reduction in disease burden is rapid but short-lived, as bioluminescent disease begins to rise within 4 days of injection. The degree of disease reduction and the subsequent delay in reaching fatal disease burden ($>2\times10^{11}$ p/sec/cm^2/sr) correlate directly with survival. Finally, RNA CAR$^+$ CTL injection resulted in significant prolongation ($p<0.01$ by log rank test of survival data) of survival compared with survival of control animals that received no CTLs and control animals that received the same dose of 2.5×10^7 RNA CAR$^+$ CTLs directed against the irrelevant antigen mesothelin (Fig. 5C). Together, these results indicate that RNA CAR$^+$ CTLs exhibit robust antitumor effects by specifically killing target cells after migration and proliferation in mice with advanced, disseminated leukemia xenografts. Importantly, we compared the survival of RNA CAR$^+$ CTLs with that of stably expressed, lentiviral generated CAR CTLs in the same Nalm-6 model. In this case, CAR CTLs were generated by lentiviral transduction to contain the same 19-BBz CAR as the RNA generated CTLs. Lentiviral CAR CTLs (10^7) were injected on day 7 after Nalm-6, based on dosing previously determined. Mice were followed as before, and median survival was not different between RNA CAR or lentiviral CAR CTLs, although one long-term survivor was seen with the persistently expressing lentiviral CAR CTLs (Fig. 5D).

Discussion

After initial challenges developing CAR T-cell therapy, improved culture systems and cell engineering technologies are leading to CAR T cells with more potent antitumor effects (Sadelain *et al.*, 2009; Kalos *et al.*, 2011; Porter *et al.*, 2011). Results from recent clinical trials indicate improved clinical results with CARs introduced with retroviral vectors (Pule *et al.*, 2008; Till *et al.*, 2008). Perhaps not surprisingly, these CAR T cells also have the potential to exhibit enhanced toxicity (Brentjens *et al.*, 2010; Morgan *et al.*, 2010; Porter *et al.*, 2011). Recent editorials have discussed the need for safer CARs (Büning *et al.*, 2010; Heslop, 2010). By combining a robust T-cell culture system (Levine *et al.*, 1997) with the

FIG. 5. Therapeutic efficacy and specificity of a single injection of RNA CAR$^+$ T cells in Nalm-6 xenograft model. **(A)** NSG mice were injected with 10^6 Nalm-6 transduced to stably express firefly luciferase, as in Supplementary Fig. S1, followed by a single tail-vein injection of 2.5×10^7 T cells electroporated with CD19-BBz or meso-BBz mRNA 7 days later (arrow). Animals were imaged at the indicated time points post injection, with total photon flux ± SE indicated on the *y*-axis; 5×10^5 p/sec/cm^2/sr represents mice with no luciferase-containing cells. $^*p<0.01$. **(B)** Photon-density heat maps of firefly luciferase-positive leukemia in representative mice at day 5 (2 days before treatment) and day 8 (24 hr post CAR$^+$ PBLs). Mice start with an equal burden of leukemia, but CD19-directed CAR$^+$ PBLs reduce disease burden by 2 logs (but do not eliminate it) as measured by photon density. **(C)** Survival of those mice treated with CD19-BBz RNA CAR$^+$ T cells is significantly prolonged compared with that of saline controls and meso-BBz CAR T cell groups. $p<0.01$ by log rank analysis. **(D)** Survival with RNA CAR CTLs compares favorably with that with lentiviral generated CAR CTLs in the same model, although no long-term survivors are noted with a single infusion of RNA CAR CTLs, consistent with our observation that single injection does not entirely eliminate disease ($n=12$, summation of two independent experiments).

optimized mRNA CAR electroporation protocol described herein, we have developed a platform that has the potential to increase the therapeutic window with CARs that contain increasingly potent signaling domains. The present findings are the first to demonstrate therapeutic effects of RNA CAR$^+$ CTLs for disseminated leukemia in a preclinical model.

A temporary expression approach toward CAR immunotherapy, such as mRNA transfection, runs counter to our previous efforts and to those of most investigators in the field. However, the improving technology for RNA transfection may complement the use of CARs that are stably expressed by integrating viral vector or transposon systems. A previous report demonstrated the feasibility of the mRNA transfection approach, achieving expression of a CD19 chimeric receptor in a natural killer cell line (Li *et al.*, 2010). RNA CAR$^+$ CTLs targeted against solid-tumor antigens have also been reported, but only in the context of intratumoral injection or *in vitro* cytotoxicity (Yoon *et al.*, 2009). Most recently, an RNA CAR CTL against CD19 was used in a peritoneal model of a CD19$^+$ tumor, where local injection resulted in a partial response (Rabinovich *et al.*, 2009). Our work extends these prior studies in several important ways, including 2-log higher surface expression and twice the *in vitro* cytotoxicity. Our data are also the first to indicate that a single injection of mRNA-transfected CAR$^+$ T cells can achieve a systemic effect, expanding and persisting sufficiently *in vivo* to migrate to distant sites of disseminated leukemia and to retain their cytotoxic effects. Massive, CAR-driven expansion of the T cells is observed during the period of CAR expression. This results in a 2-log reduction of leukemic burden and extended survival an aggressive xenograft model characterized by rapid human ALL engraftment. Importantly, the survival of mice bearing xenografted leukemia and administered a single injection of RNA CAR CTLs is comparable to survival achieved by stable lentivirus CAR CTLs. The sites and timing of relapse are similar between these groups, although only stable expressed CARs result in long-term cures (>180 days). Survival in the RNA CAR model is directly correlated with degree the of initial disease reduction, although the periodontal and paraspinal regions remain the first sites of relapse in both RNA and lentiviral CAR models (Supplementary Fig. S2).

Adverse events, quite possibly from cytokine release, have been observed in early clinical trials (Brentjens *et al.*, 2010; Morgan *et al.*, 2010). CARs that incorporate costimulatory domains such as CD28 and 4-1BB mediate increased cytokine release upon antigen triggering (Maher *et al.*, 2002; Carpenito *et al.*, 2009; Milone *et al.*, 2009). Our finding that CAR surface expression is relatively mRNA dose-independent, with resulting relatively mRNA dose-dependent IFN-γ and IL-2 cytokine secretion over time, raises the future possibility of tailoring expression levels to mitigate the release of cytokines that may result in toxicity. Other toxicities encountered with stably transduced CAR T cells have been on-target/off-organ effects, such as the expected depletion of normal B cells following CD19 CAR therapy, or the induction of hepatic toxicity following carbonic anhydrase IX therapy (Lamers *et al.*, 2006). Although not tested in these studies, it is likely that repeated administration of RNA CARs would be required to elicit this form of toxicity. Finally, concerns over the lentiviral or retroviral introduction of CARs into CTLs include the theoretical possibilty of malignant transformation from insertional mutagenesis, a subject of significant regulatory oversight even for mature T cells (Nienhuis *et al.*, 2006; Bushman, 2007). As there is no integration into the host-cell genome and the CAR expression is self-limited, these concerns are potentially circumvented by mRNA transfection. Also, importantly, as RNA-expressed CARs seem to function similarly to stably expressed CARs both *in vitro* and *in vivo* in preclinical animal models in the short term, this platform provides a potentially more rapid way to evaluate iterations in CAR design that could be translated back to the stable expression systems.

There are several potential limitations of RNA CAR therapy. The principal limitation is the short-term expression, currently limited to about 1 week. We found that the Nalm-6 xenograft was affected much more rapidly than we expected, with a 2-log reduction in tumor load within 1 day of RNA CAR administration. Nevertheless, it will likely be necessary to dose repeatedly with RNA CARs for therapeutic efficacy, and further study is under way to test this strategy. Given the current observations in ongoing clinical trials that persistence of transferred mature lymphocytes is poor, repeated infusions may be necessary whether the CAR is transient or stable until methods to improve T-cell persistence are developed and tested. Another limitation is that the xenograft model used for these experiments is best suited for assessing efficacy, not toxicity, although no overt toxicity to the animals was observed. Further testing, including testing different RNA and T-cell doses and how they relate to the potential for cytokine release, remains to be done now that basic efficacy has been demonstrated. It is reassuring that the data with our RNA CAR CTLs show all the target-based cytotoxic properties of their lentiviral counterparts (Carpenito *et al.*, 2009; Milone *et al.*, 2009). The RNA CAR CTLs exhibited antigen specificity with concomitant ability to migrate to and expand at sites of disseminated leukemia after a single intravenous injection. Trafficking of CAR CTLs to sites of disease is critical to their antitumor function, as has been demonstrated in a prostate cancer xenograft model, and our work is the first to demonstrate that CD19 RNA CAR CTLs can traffic to and function at all sites of disseminated leukemia after a single tail-vein injection (Dobrenkov *et al.*, 2008). Importantly, we demonstrate that RNA CARs are still expressed at high levels after circulation and expansion in a tumor-bearing xenograft, indicating functional CTLs despite potential receptor internalization and dilution of RNA from proliferation after antigen engagement.

There are several potential opportunities for RNA CAR CTL therapy. First, RNA CARs offer a potential strategy for toxicity mitigation (self-limited expression) that is not possible with stably expressed CARs, with the possible exception of the incorporation of suicide systems with stably expressed CARs (Marktel *et al.*, 2003; Sato *et al.*, 2007). Second, RNA CARs offer the potential to accelerate the pace of CAR development, by providing a flexible and more rapid path to the clinic, and thereby enable an efficient iterative approach to optimize CAR design and potency. The regulatory approval process has the potential to be less cumbersome with RNA CARs than with stably expressed CARs that require genomic integration. Clinical grade mRNA is far less costly to produce than integrating retroviral or lentiviral vectors, and somewhat more expensive than plasmid DNA that is being used in transfection- or transposon-based protocols (Singh *et al.*, 2008; Till *et al.*, 2008). How the true

cost-effectiveness plays out will ultimately be determined by the number of T cells, number of infusions, and duration of response—factors not yet known. Finally, it may be attractive to combine RNA CAR "knock down" therapy, using potent but potentially toxic CARs for remission induction, with consolidation and maintenance therapy using stably expressed CARs as a strategy to provide memory CAR^+ cells.

In summary, a short-term expression platform that we have developed provides an addition alternative for cell therapy and may have advantages for certain applications; with repeated infusions over time, it may be possible to achieve long-term disease control or eradication of otherwise treatment-resistant leukemia. The optimal schedule for such infusions and their feasibility for human use remain to be determined, but these early data support continued pursuit of this technology.

Acknowledgments

This work was supported in part by research grants R01CA120409 and P01CA066726 (C.H.J.) and R01CA102646 (S.A.G.) and by Weinberg, Cookies for Kids, and W.W. Smith Foundation grants (S.A.G.). D.M.B. designed the research, performed the experiments, interpreted the data, and wrote the paper. X.L. and S.J. performed research. C.C., M.K., and R.G.C. designed the research and interpreted the data. S.A.G, Y.Z., and C.H.J. designed the research, and wrote the paper.

Author Disclosure Statement

C.H.J. has patent applications in some of the technology described in this article. All other authors have no conflict of interest.

References

Betts, M.R., and Koup, R.A. (2004). Detection of T-cell degranulation: CD107a and b. Methods Cell Biol. 75, 497–512.

Birkholz, K., Hombach, A., Krug, C., *et al.* (2009). Transfer of mRNA encoding recombinant immunoreceptors reprograms $CD4^+$ and $CD8^+$ T cells for use in the adoptive immunotherapy of cancer. Gene Ther. 16, 596–604.

Brentjens, R. J., Santos, E., Nikhamin, Y., *et al.* (2007). Genetically targeted T cells eradicate systemic acute lymphoblastic leukemia xenografts. Clin. Cancer Res. 13(18 Pt 1), 5426–5435.

Brentjens, R., Yeh, R., Bernal, Y., *et al.* (2010). Treatment of chronic lymphocytic leukemia with genetically targeted autologous T cells: case report of an unforeseen adverse event in a phase I clinical trial. Mol. Ther. 18, 666–668.

Brocker, T., and Karjalainen, K. (1998). Adoptive tumor immunity mediated by lymphocytes bearing modified antigen-specific receptors. Adv. Immunol. 68, 257–269.

Büning, H., Uckert, W., Cichutek, K., *et al.* (2010). Do CARs need a driver's license? Adoptive cell therapy with chimeric antigen receptor-redirected T cells has caused serious adverse events. Hum. Gene Ther. 21, 1039–1042.

Bushman, F.D. (2007). Retroviral integration and human gene therapy. J. Clin. Invest. 117, 2083–2086.

Carpenito, C., Milone, M.C., Hassan, R., *et al.* (2009). Control of large, established tumor xenografts with genetically retargeted human T cells containing CD28 and CD137 domains. Proc. Natl. Acad. Sci. U.S.A. 106, 3360–3365.

Cheadle, E.J., Hawkins, R.E., Batha, H., *et al.* (2010). Natural expression of the CD19 antigen impacts the long-term engraftment but not antitumor activity of CD19-specific engineered T cells. J. Immunol. 184, 1885–1896.

Deeks, S.G., Wagner, B., Anton, P.A., *et al.* (2002). A phase II randomized study of HIV-specific T-cell gene therapy in subjects with undetectable plasma viremia on combination antiretroviral therapy. Mol. Ther. 5, 788–797.

Dobrenkov, K., Olszewska, M., Likar, Y., *et al.* (2008). Monitoring the efficacy of adoptively transferred prostate cancer-targeted human T lymphocytes with PET and bioluminescence imaging. J. Nucl. Med. 49, 1162–1170.

Eshhar, Z. (1997). Tumor-specific T-bodies: towards clinical application. Cancer Immunol. Immunother. 45, 131–136.

Eshhar, Z., Waks, T., Gross, G., and Schindler, D.G. (1993). Specific activation and targeting of cytotoxic lymphocytes through chimeric single chains consisting of antibody-binding domains and the γ or ζ subunits of the immunoglobulin and T-cell receptors. Proc. Natl. Acad. Sci. U.S.A. 90, 720–724.

Hacein-Bey-Abina, S., Garrigue, A., Wang, G.P., *et al.* (2008). Insertional oncogenesis in 4 patients after retrovirus-mediated gene therapy of SCID-X1. J. Clin. Invest. 118, 3132–3142.

Hermans, I.F., Silk, J.D., Yang, J., *et al.* (2004). The VITAL assay: a versatile fluorometric technique for assessing CTL- and NKT-mediated cytotoxicity against multiple targets in vitro and in vivo. J. Immunol. Methods 285, 25–40.

Heslop, H. (2010). Safer CARS. Mol. Ther. 18, 661–662.

Horowitz, M.M., Gale, R.P., Sondel, P.M., *et al.* (1990). Graft-versus-leukemia reactions after bone marrow transplantation. Blood 75, 555–562.

Imai, C., Mihara, K., Andreansky, M., *et al.* (2004). Chimeric receptors with 4-1BB signaling capacity provoke potent cytotoxicity against acute lymphoblastic leukemia. Leukemia 18, 676–684.

James, S.E., Greenberg, P.D., Jensen, M.C., *et al.* (2010). Mathematical modeling of chimeric TCR triggering predicts the magnitude of target lysis and its impairment by TCR down-modulation. J. Immunol. 184, 4284–4294.

Kalchenko, V., Shivtiel, S., Malina, V., *et al.* (2006). Use of lipophilic near-infrared dye in whole-body optical imaging of hematopoietic cell homing. J. Biomed. Opt. 11, 050507.

Kalos, M., Levine, B.L., Porter, D.L., *et al.* (2011). T cells with chimeric antigen receptors have potent antitumor effects and can establish memory in patients with advanced leukemia. Sci. Transl. Med. 3, 95ra73.

Kershaw, M.H., Westwood, J.A., Parker, L.L., *et al.* (2006). A phase I study on adoptive immunotherapy using gene-modified T cells for ovarian cancer. Clin. Cancer Res. 12(20 Pt 1), 6106–6115.

Lamers, C.H., Sleijfer, S., Vulto, A.G., *et al.* (2006). Treatment of metastatic renal cell carcinoma with autologous T-lymphocytes genetically retargeted against carbonic anhydrase IX: first clinical experience. J. Clin Oncol. 24, e20–e22.

Levine, B.L., Bernstein, W.B., Connors, M., *et al.* (1997). Effects of CD28 costimulation on long-term proliferation of CD4+ T cells in the absence of exogenous feeder cells. J. Immunol. 159, 5921–5930.

Li, L., Liu, L.N., Feller, S., *et al.* (2010). Expression of chimeric antigen receptors in natural killer cells with a regulatory-compliant non-viral method. Cancer Gene. Ther. 17, 147–154.

Maher, J., Brentjens, R.J., Gunset, G., *et al.* (2002). Human T-lymphocyte cytotoxicity and proliferation directed by a single chimeric TCRzeta/CD28 receptor. Nat. Biotechnol. 20, 70–75.

Malone, R.W., Felgner, P.L., and Verma, I.M. (1989). Cationic liposome-mediated RNA transfection. Proc. Natl. Acad. Sci. U.S.A. 86, 6077–6081.

Marktel, S., Magnani, Z., Ciceri, F., *et al.* (2003). Immunologic potential of donor lymphocytes expressing a suicide gene for early immune reconstitution after hematopoietic T-cell-depleted stem cell transplantation. Blood 101, 1290–1298.

Masters, J.R., Thomson, J.A., Daly-Burns, B., *et al.* (2001). Short tandem repeat profiling provides an international reference standard for human cell lines. Proc. Natl. Acad. Sci. U.S.A. 98, 8012–8017.

Mehta, J. (1993). Graft-versus-leukemia reactions in clinical bone marrow transplantation. Leuk. Lymphoma 10, 427–432.

Milone, M.C., Fish, J.D., Carpenita, C., *et al.* (2009). Chimeric receptors containing CD137 signal transduction domains mediate enhanced survival of T cells and increased antileukemic efficacy *in vivo*. Mol. Ther. 17, 1453–1464.

Morgan, R.A., Yang, J.C., Kitano, M., *et al.* (2010). Case report of a serious adverse event following the administration of T cells transduced with a chimeric antigen receptor recognizing ERBB2. Mol. Ther. 18, 843–851.

Nadler, L.M., Anderson, K.C., Marti, G., *et al.* (1983). B4, a human B lymphocyte-associated antigen expressed on normal, mitogen-activated, and malignant B lymphocytes. J. Immunol. 131, 244–250.

Nienhuis, A.W., Dunbar, C.E., and Sorrentino, B.P. (2006). Genotoxicity of retroviral integration in hematopoietic cells. Mol. Ther. 13, 1031–1049.

Pinthus, J.H., Waks, T., Malina, V., *et al.* (2004). Adoptive immunotherapy of prostate cancer bone lesions using redirected effector lymphocytes. J. Clin. Invest. 114, 1774–1781.

Plosker, G.L., and Figgitt, D.P. (2003). Rituximab: a review of its use in non-Hodgkin's lymphoma and chronic lymphocytic leukaemia. Drugs 63, 803–843.

Porter, D.L., Levine, B.L., Kalos, M., *et al.* (2011). Chimeric antigen receptor-modified T cells in chronic lymphoid leukemia. N. Engl. J. Med. [Epub ahead of print]

Pule, M.A., Savoldo, B., Myers, G.D., *et al.* (2008). Virus-specific T cells engineered to coexpress tumor-specific receptors: persistence and antitumor activity in individuals with neuroblastoma. Nat. Med. 14, 1264–1270.

Rabinovich, P.M., Komarovskaya, M.E., Wrzesinski, S.H., *et al.* (2009). Chimeric receptor mRNA transfection as a tool to generate antineoplastic lymphocytes. Hum. Gene Ther. 20, 51–61.

Sadelain, M., Brentjens, R., and Rivière, I. (2009). The promise and potential pitfalls of chimeric antigen receptors. Curr. Opin. Immunol. 21, 215–223.

Sato, T., Neschadim, A., Konrad, M., *et al.* (2007). Engineered human tmpk/AZT as a novel enzyme/prodrug axis for suicide gene therapy. Mol.Ther. 15, 962–970.

Shaffer, D.R., Savoldo, B., Yi, Z., *et al.* (2011). T cells redirected against CD70 for the immunotherapy of CD70-positive malignancies. Blood 117, 4304–4314.

Singh, H., Manuri, P.R., Olivares, S., *et al.* (2008). Redirecting specificity of T-cell populations for CD19 using the Sleeping Beauty system. Cancer Res. 68, 2961–2971.

Suhoski, M.M., Golovina, T.N., Aqui, N.A., *et al.* (2007). Engineering artificial antigen-presenting cells to express a diverse array of co-stimulatory molecules. Mol. Ther. 15, 981–988.

Teachey, D.T., Obzut, D.A., Cooperman, J., *et al.* (2006). The mTOR inhibitor CCI-779 induces apoptosis and inhibits growth in preclinical models of primary adult human ALL. Blood 107, 1149–1155.

Teachey, D.T., Sheen, C., Hall, J., *et al.* (2008). mTOR inhibitors are synergistic with methotrexate: an effective combination to treat acute lymphoblastic leukemia. Blood 112, 2020–2023.

Till, B.G., Jensen, M.C., Wang, J., *et al.* (2008). Adoptive immunotherapy for indolent non-Hodgkin lymphoma and mantle cell lymphoma using genetically modified autologous CD20-specific T cells. Blood 112, 2261–2271.

van Vollenhoven, R.F., Emery, P., Bingham, C.O. 3rd, *et al.* (2010). Longterm safety of patients receiving rituximab in rheumatoid arthritis clinical trials. J. Rheumatol. 37, 558–567.

Yoon, S.H., Lee, J.M., Cho, H.I., *et al.* (2009). Adoptive immunotherapy using human peripheral blood lymphocytes transferred with RNA encoding Her-2/neu-specific chimeric immune receptor in ovarian cancer xenograft model. Cancer Gene Ther. 16, 489–497.

Zhao, H., Doyle, T.C., Coquoz, O., *et al.* (2005). Emission spectra of bioluminescent reporters and interaction with mammalian tissue determine the sensitivity of detection in vivo. J. Biomed. Opt. 10, 41210.

Zhao, Y., Zheng, Z., Robbins, P.F., *et al.* (2005). Primary human lymphocytes transduced with NY-ESO-1 antigen-specific TCR genes recognize and kill diverse human tumor cell lines. J. Immunol. 174, 4415–4423.

Zhao, Y., Zheng, Z., Cohen, C.J., *et al.* (2006). High-efficiency transfection of primary human and mouse T lymphocytes using RNA electroporation. Mol. Ther. 13, 151–159.

Address correspondence to:
Dr. Carl H. June
Abramson Family Cancer Research Institute
University of Pennsylvania Cancer Center
Philadelphia, PA 19104

E-mail: cjune@exchange.upenn.edu

Received for publication May 11, 2011;
accepted after revision August 12, 2011.

Published online: August 12, 2011.